

A VARIABLE EFFICIENCY FOR THIN-DISK BLACK HOLE ACCRETION

CHRISTOPHER S. REYNOLDS¹

Joint Institute for Laboratory Astrophysics, Campus Box 440, University of Colorado, Boulder, CO 80309

AND

PHILIP J. ARMITAGE

School of Physics and Astronomy, University of St. Andrews, Fife KY16 9SS, UK

Received 2001 July 3; accepted 2001 September 26; published 2001 October 12

ABSTRACT

We explore the presence of torques at the inner edges of geometrically thin black hole accretion disks using three-dimensional MHD simulations in a pseudo-Newtonian potential. By varying the saturation level of the magnetorotational instability that leads to angular momentum transport, we show that the dynamics of gas inside the radius of marginal stability varies depending upon the magnetic field strength just *outside* that radius. Weak fields are unable to causally connect material within the plunging region to the rest of the disk, and zero torque is an approximately correct boundary condition at the radius of marginal stability. Stronger fields, which we obtain artificially but which may occur physically within more complete disk models, are able to couple at least some parts of the plunging region to the rest of the disk. In this case, angular momentum (and implicitly energy) is extracted from the material in the plunging region. Furthermore, the magnetic coupling to the plunging region can be highly time dependent with large fluctuations in the torque at the radius of marginal stability. This implies varying accretion efficiencies, both across systems and within a given system at different times. The results suggest a possible link between changes in X-ray and outflow activity, with both being driven by transitions between weak and strong field states.

Subject headings: accretion, accretion disks — black hole physics — hydrodynamics — instabilities — MHD

1. INTRODUCTION

In a wide class of black hole systems, including quasars, Seyfert galaxies, and high-state Galactic black hole candidates, the accretion disk is almost certainly geometrically thin and radiatively efficient. The radiation emitted from an annulus of such a disk does not simply equal the change in gravitational binding energy as gas flows across the annulus, but rather it includes a contribution from energy transported into the annulus from elsewhere in the disk. As a consequence, the disk structure, along with related quantities such as the radiative efficiency (the fraction of rest mass energy that is radiated during the accretion process), depends upon the location and nature of the boundary conditions at the inner disk edge.

For a black hole accretion disk, a natural location to place the inner boundary condition is at the radius of marginal stability, $r = r_{\text{ms}}$. This is the radius inside of which circular orbits are no longer stable, and it is at $6GM/c^2$ for a nonrotating (Schwarzschild) black hole. In the standard model for black hole accretion (Novikov & Thorne 1973; Paczyński & Bisnovaty-Kogan 1981; Abramowicz & Kato 1989; Paczyński 2000), one assumes that there is no angular momentum transport across $r = r_{\text{ms}}$. The motivation for this zero-torque boundary condition (ZTBC) is that the radial flow rapidly becomes supersonic once inside $r = r_{\text{ms}}$, and so the material loses causal contact with the rest of the disk. Thereafter, material simply spirals ballistically into the black hole. For this reason we will refer to the region where $r < r_{\text{ms}}$ as the plunging region.

The ZTBC limits the accretion efficiency to around 6% (for a nonrotating black hole)—already a substantial figure. However, it is possible that even higher efficiencies may arise. The suggestion is that magnetic fields, which are generated in the disk by the magnetorotational instability (Balbus & Hawley

1991), may become dynamically significant within the plunging region. These fields could then causally connect the plunging region to the rest of the accretion disk, allowing energy and angular momentum to be extracted from gas as it executes its final spiral into the black hole (Krolik 1999; Gammie 1999; Agol & Krolik 2000). Subsequent numerical simulations (none of which are general relativistic) have confirmed the presence of magnetic torques at the marginally stable orbit but have reached different conclusions as to their impact on the dynamics of the flow. Global MHD simulations of adiabatic accretion tori (Hawley 2000; Hawley & Krolik 2001) showed outward angular momentum transport continuing within r_{ms} , while unstratified simulations suggested more modest effects (Armitage, Reynolds, & Chiang 2001; Hawley 2001). The important parameters or numerical differences that cause this different behavior remain to be determined.

In this Letter we explore the suggestion (C. Gammie 2000, private communication) that the dynamics of the flow within the plunging region may depend upon the strength of magnetic fields in the disk at $r > r_{\text{ms}}$. We extend our earlier work by presenting “boosted” simulations in which the strength of the magnetic field in the saturated turbulence is enhanced by starting with an initially large seed field. This is a numerical trick, although it may have a physical counterpart if the inner disk is threaded by a large-scale magnetic field. For the purposes of this Letter, however, the aim is solely to allow us to study how the dynamics of the plunging region vary with field strength in a controlled fashion. We show that the dynamics of gas in the plunging region and the validity of the ZTBC do indeed depend upon the saturation field strength, and we discuss the implications for observations of accreting black holes.

2. SIMULATIONS

We use the ZEUS code to solve the equations of ideal MHD (Stone & Norman 1992a, 1992b; Clarke, Norman, & Fielder

¹ Present address: Department of Astronomy, University of Maryland, College Park, MD 20742.

TABLE 1
THE SET OF SIMULATIONS

Run Number (1)	ϕ_{\max} (2)	z_{\max}/r_{Sch} (3)	n_r (4)	n_ϕ (5)	n_z (6)	β_i (7)
1	$\pi/4$	0.5	200 (40)	60	40	5000 (z)
2	$\pi/4$	0.5	200 (40)	60	40	500 (z)
3	$\pi/4$	0.5	200 (40)	60	40	100 (ϕ)
4	$\pi/2$	0.5	200 (40)	120	40	5000 (z)

NOTE.—Col. (1): run numbers. Col. (2) ϕ domain. Col. (3): z domain. Col. (4): number of radial cells (and number inside $r = r_{\text{ms}}$). Col. (5): number of ϕ cells. Col. (6): number of vertical cells. Col. (7): initial β of plasma (and direction).

1994; Norman 2000) in cylindrical coordinates, using a setup very similar to that described previously (Armitage et al. 2001). Stated briefly, the computational domain is the wedge given by $r \in (r_{\text{in}}, r_{\text{out}})$, $\phi \in (0, \phi_{\max})$, and $z \in (-z_{\max}, z_{\max})$. The effects of general relativity (in particular the existence of an innermost stable orbit) are modeled in this inherently nonrelativistic code by using a pseudo-Newtonian potential (Paczynski & Wiita 1980), $\Phi = -GM/(r - r_{\text{Sch}})$, where $r_{\text{Sch}} = 2GM/c^2$. The vertical component of gravity is neglected, so the disk has no vertical structure. There is therefore no time-averaged variation of density or magnetic field strength with z . The equation of state is isothermal, with a sound speed c_s that is assumed uniform and constant. At r_{ms} , the ratio of the sound speed to the Keplerian velocity is $c_s/v_\phi = 0.065$, slightly cooler than our previous simulations.

The initial conditions for density and velocity were obtained by relaxing a Gaussian radial density profile, using ZEUS in its one-dimensional hydrodynamic mode, to produce a density profile that is in accurate numerical equilibrium. The initial configurations of the three-dimensional MHD simulations were then produced by adding a seed magnetic field. Table 1 shows the computational domain, resolution, initial value of β , and seed field configuration for the simulations. As usual, β is defined as the ratio of thermal energy density to magnetic energy density. In all cases, we set $r_{\text{in}} = 4GM/c^2$ and $r_{\text{out}} = 20GM/c^2$. The radial boundary conditions were such as to permit outflow, and all other boundaries were made periodic. These simulations were then evolved until the magnetorotational instability (MRI) became nonlinear and produced fully developed MHD turbulence (in the sense that the MRI has saturated and there is no further long-term growth of the magnetic energy). This turbulence drives accretion of material through the inner radial boundary, and the

run is continued until an appreciable amount of material has left the computational domain.

3. THE DYNAMICS OF THE FLOW WITHIN THE PLUNGING REGION

3.1. Time-averaged Properties

We consider first the time-averaged properties of our runs. Figure 1 shows time-averaged radial profiles for β^{-1} (i.e., the ratio of magnetic field energy density to thermal energy density) and the specific angular momentum l . As intended, the magnetic field in run 2, which starts with a relatively strong vertical seed field ($\beta_z = 500$), saturates with significantly higher relative magnetic field energy than those runs that start with either a weaker initial field or a comparable toroidal field. This is due to the continued boosting of the MRI from the conserved vertical flux that accompanies the initial vertical field (Hawley, Gammie, & Balbus 1995). Increasing the size of the computational domain also increases the saturation value of the magnetic field, but by a smaller factor.

The dynamics of the flow—diagnosed using the specific angular momentum—correlate with the saturation field strength. First, consider the unboosted runs (runs 1, 3, and 4; Fig. 1, *solid, dashed, and dot-dashed lines, respectively*). As one approaches and enters the plunging region, the radial profile of l flattens. If the ZTBC is strictly valid, l should be constant within the plunging region. For these runs, we obtain the same result as before (Armitage et al. 2001), namely, that the ZTBC yields a good but not perfect description of the inner disk dynamics. Indeed, examination of the $r\phi$ component of the magnetic stress tensor shows that the Maxwell stresses at $r = r_{\text{ms}}$ do not vanish but are less than the peak stress, which occurs at $r \sim (10\text{--}12)GM/c^2$, by a factor of 5–8.

On the other hand, angular momentum transport within the plunging region is much more significant in the boosted run (run 2; Fig. 1, *dotted line*). The time-averaged stress at $r = r_{\text{ms}}$ is still less than the peak value (which occurs at $r \sim 8GM/c^2$), but by a factor of only 2. Significant stresses continue to operate within the region $r < r_{\text{ms}}$, and there is evidently a clear violation of the ZTBC.

3.2. Variability within Individual Simulations

Turbulent accretion disks are inherently variable systems and so it is also interesting to examine variability during our sim-

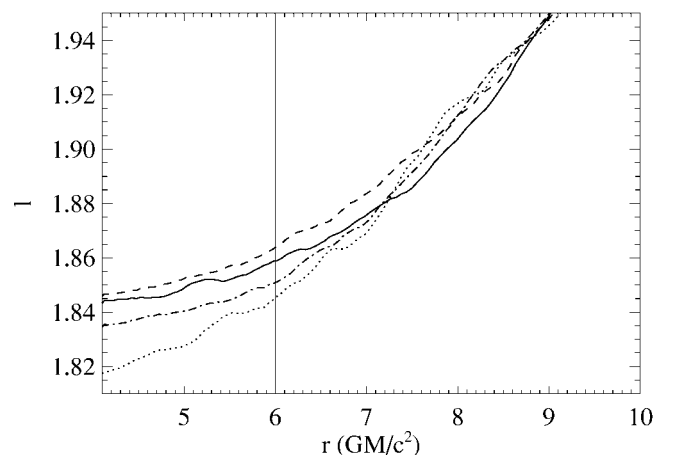
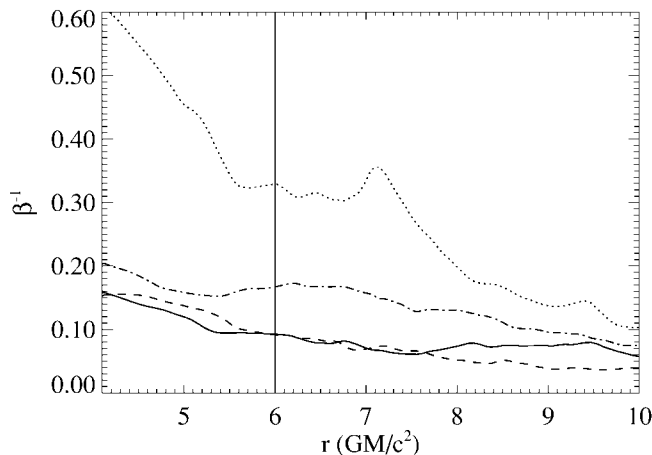


FIG. 1.—Time-averaged radial profiles of β^{-1} (ratio of magnetic energy density to thermal energy density) and l (specific angular momentum) for our high-resolution simulations. The runs are denoted as follows: run 1 (*solid line*), run 2 (*dotted line*), run 3 (*dashed line*), and run 4 (*dot-dashed line*).

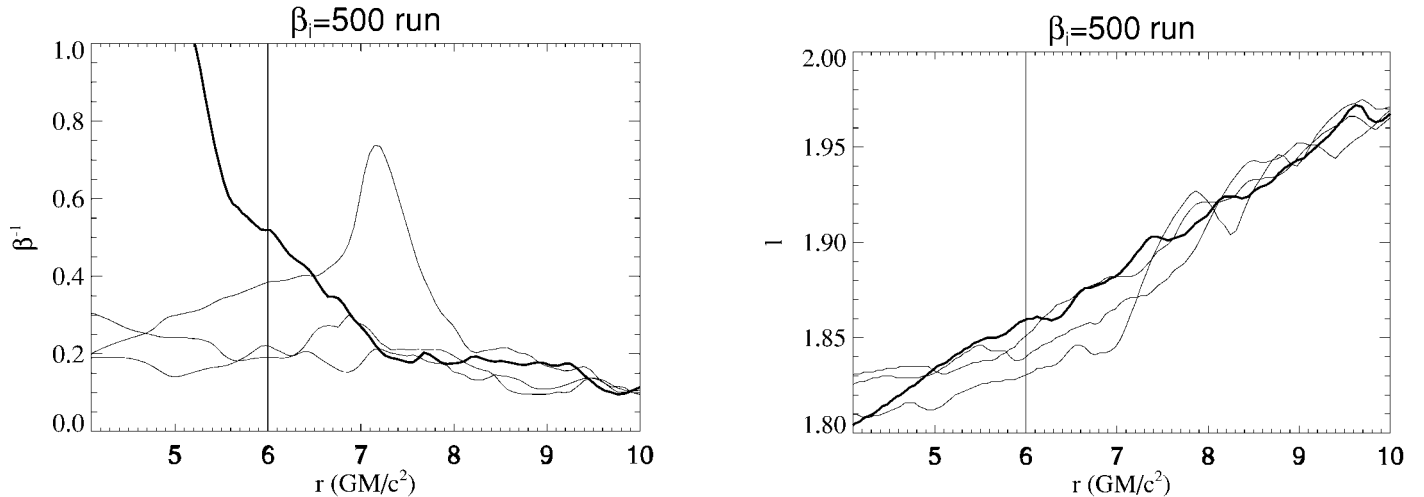


FIG. 2.—Radial profiles of β^{-1} and l for individual time slices from the boosted simulation, run 2. In particular, note the anomalous event (*thick lines*) during which the plunging region becomes magnetically dominated and there is efficient angular momentum transport out of this region.

ulations. For this purpose, we will compare and contrast run 1 and run 2. Both runs display order unity temporal and spatial fluctuations in β^{-1} . For the unboosted run these fluctuations have only a small effect on l . For the boosted run shown in Figure 2, however, there are much larger fluctuations in l . In particular, during one time slice from run 2, a large part of the plunging region becomes magnetically dominated ($\beta < 1$). During this period (Fig. 2, *thick lines*), l declines within the plunging region with the same slope as in the rest of the disk, with the Maxwell stresses staying fairly constant well into the plunging region. Events as dramatic as this are fairly rare (caught in one out of the 12 independent time slices that we analyzed), but it is clear that the stress at $r = r_{\text{ms}}$ is a rapidly varying function of time, with much more frequent occurrences of moderate stress.

Extraction of energy and angular momentum from within the plunging region can occur only if the material can remain causally connected to the rest of the disk. Analysis of the simulations shows that large stresses occur within the plunging region when the magnetic fields are strong enough for the *peak* radial MHD wave speed to exceed the radial inflow velocity throughout a large part of the plunging region. It is worth noting that even during the magnetically dominated event seen in run 2, the *azimuthally averaged* MHD wave speeds are always slower than the inflow speeds. The angular momentum transport within this highly inhomogeneous plasma therefore appears to be mediated by low- β (i.e., higher relative magnetic field) filaments.

4. DISCUSSION

4.1. Radiative Efficiency

Calculating the implied change to the radiative efficiency as a consequence of the magnetic torque at r_{ms} is not straightforward (see the discussion in Hawley & Krolik 2001). A simple approach is to note that the dissipation rate is

$$Q(r) = \left| \frac{d\Omega}{d \ln r} \right| \int T^{r\phi} dz, \quad (1)$$

where $T^{r\phi}$ is the local stress. We can then estimate the change in the radiative efficiency by comparing $Q(r)$, computed using the stress measured in the simulations, with the form expected in a steady disk if there were no stress at r_{ms} .

In practice, the nonsteady nature of the flow and the limited radial extent of the simulations create difficulties. An indicative estimate, however, follows from noting that in run 2 the mean magnetic stress is roughly constant between r_{ms} and $2r_{\text{ms}}$. Compared to a standard disk model, this implies a 50% increase in the dissipation in the region $r_{\text{ms}} < r < 2r_{\text{ms}}$ and a 10% increase over $r_{\text{ms}} < r < 10r_{\text{ms}}$. Significantly larger effects are seen in some individual time slices.

4.2. Comparison with Previous Work

The simulations presented here suggest that the different dynamics within the plunging region, obtained by Hawley & Krolik (2001) and Armitage et al. (2001), are plausibly due to different values in the saturation levels of magnetic fields in the disk. The relatively strong magnetic fields in the former simulations, which obtained $\beta \sim 5$ –10, are more comparable to the boosted simulations in the current work and lead to substantial angular momentum transport within the plunging region. Weaker disk fields, with $\beta \sim 20$ and a Shakura & Sunyaev (1973) α parameter of $\alpha \sim 0.02$ –0.04, produce much less striking effects. Although there are undoubtedly other significant differences between the simulations, all work to date is broadly consistent with the hypothesis that significant magnetic coupling to the plunging region requires disk fields with $\alpha \sim 0.1$ (and $\beta \sim 10$). This applies for disks that are moderately thin, with relative thickness $h/r \sim 0.1$, which are the only systems that have been simulated so far.

4.3. Scaling to Thinner Disks

Very thin disks are difficult to simulate, and it is not obvious how the threshold β seen in the current work scales with h/r . We note, however, that the Alfvén speed in the disk scales as $v_A \propto (h/r) \beta^{-1/2}$. Unless β in the disk decreases rapidly with decreasing h/r , the Alfvén speed in the gas immediately outside the plunging region will decrease with decreasing disk thickness. Conversely, the inflow speed v_r within the plunging region is a fixed function of r and is independent of h/r . Hence, a larger increase in the Alfvén speed is needed if thinner disks are to maintain causal contact into the plunging region. It is therefore probable that it becomes increasingly more difficult to extract energy from the plunging region as the disk becomes thinner, although further simulation work is required before drawing robust conclusions.

5. CONCLUSIONS

In this Letter we have used MHD simulations to investigate the effect of the magnetic field strength in the body of the accretion disk on the dynamics of the material within the plunging region. For a disk with a sound speed corresponding to $h/r \approx 0.1$, we find that plausible saturation values of the magnetic field are within a factor of a few of a threshold between two regimes. In the runs that saturated with a fairly low magnetic field ($\beta \sim 20$), there was only modest extraction of angular momentum from material within the plunging region, and the ZTBC was a reasonable approximation. In our “boosted” runs, where the field saturated at a higher level ($\beta \sim 5\text{--}10$), we found significantly stronger angular momentum transport within the plunging region. Furthermore, our boosted run showed sporadic intervals of very efficient angular momentum transport (with stresses that remained fairly constant well within the plunging region). We note that stratified simulations by other authors (Hawley 2000; Miller & Stone 2000; Hawley & Krolik 2001) suggest that magnetic fields could be stronger (i.e., lower β) above the disk midplane. Such fields, which are not included in our simulations, could contribute to more significant transport within the plunging region.

The extraction of energy and angular momentum from ma-

terial in the plunging region can significantly increase the efficiency of accretion above the standard value, especially in the innermost regions. This raises the possibility of varying efficiencies, both across systems and within a given system at different times.

In this Letter we have used a large-scale flux threading the accretion disk as a numerical device for altering the saturation level of the MRI. Large-scale fields could also, of course, be present in real systems and are often invoked in models for the formation of jets and outflows (e.g., Ouyed, Pudritz, & Stone 1997 and references therein). This raises the interesting possibility that periods of increased luminosity (due to a high radiative efficiency) may be related to periods during which strong outflows occur. Such associations have been reported for Galactic black hole candidates such as GRS 1915+105 (Mirabel et al. 1998).

We extend a special thanks to Charles Gammie for suggesting this problem. We are grateful to the developers of ZEUS and ZEUS-MP for making these codes available as community resources. C. S. R. acknowledges support from Hubble Fellowship grant HF-01113.01-98A. We also thank the NSF for support under grant AST 98-76887. P. J. A. thanks JILA for hospitality.

REFERENCES

- Abramowicz, M. A., & Kato, S. 1989, *ApJ*, 336, 304
 Agol, E., & Krolik, J. H. 2000, *ApJ*, 528, 161
 Armitage, P. J., Reynolds, C. S., & Chiang, J. 2001, *ApJ*, 548, 868
 Balbus, S. A., & Hawley, J. F. 1991, *ApJ*, 376, 214
 Clarke, D. A., Norman, M. L., & Fiedler, R. A. 1994, National Center for Supercomputing Applications Tech. Rep. 15
 Gammie, C. F. 1999, *ApJ*, 522, L57
 Hawley, J. F. 2000, *ApJ*, 528, 462
 ———. 2001, *ApJ*, 554, 534
 Hawley, J. F., Gammie, C. F., & Balbus, S. A. 1995, *ApJ*, 440, 742
 Hawley, J. F., & Krolik, J. H. 2001, *ApJ*, 548, 348
 Krolik, J. H. 1999, *ApJ*, 515, L73
 Miller, K. A., & Stone, J. M. 2000, *ApJ*, 534, 398
 Mirabel, I. F., et al. 1998, *A&A*, 330, L9
 Norman, M. L. 2000, *Rev. Mexicana Astron. Astrofis. Ser. Conf.*, 9, 66
 Novikov, I. D., & Thorne, K. S. 1973, in *Black Holes—Les Astres Occlus*, ed. S. DeWitt & B. DeWitt (New York: Gordon and Breach), 345
 Ouyed, R., Pudritz, R. E., & Stone, J. M. 1997, *Nature*, 385, 409
 Paczyński, B. 2000, preprint (astro-ph/0004129)
 Paczyński, B., & Bisnovatyi-Kogan, G. 1981, *Acta. Astron.*, 31, 283
 Paczyński, B., & Wiita, P. J. 1980, *A&A*, 88, 23
 Shakura, N. I., & Sunyaev, R. A. 1973, *A&A*, 24, 337
 Stone, J. M., & Norman, M. L. 1992a, *ApJS*, 80, 791
 ———. 1992b, *ApJS*, 80, 819